J|A|C|S
ARTICLES
Published on Web 12/15/2006

High Fidelity Functional Patterns of an Extracellular Matrix Protein by Electron Beam-Based Inactivation

Jonas Rundqvist,[†] Beatriz Mendoza,[†] Jeffrey L. Werbin,[‡] William F. Heinz,[‡] Christopher Lemmon,[§] Lewis H. Romer,[§] David B. Haviland,*[,†] and Jan H. Hoh*[,‡]

Contribution from Nanostructure Physics, Royal Institute of Technology, AlbaNova University Center, Roslagsvägen 30B, SE-106 91 Stockholm, Sweden, and Departments of Physiology and Anesthesiology, Johns Hopkins School of Medicine, 725 North Wolfe Street, Baltimore, Maryland 21205

Received June 7, 2006; E-mail: jhoh@jhmi.edu; haviland@nanophys.kth.se

Abstract: Controlling the organization of proteins on surfaces provides a powerful biochemical tool for determining how cells interpret the spatial distribution of local signaling molecules. Here, we describe a general high fidelity approach based on electron beam writing to pattern the functional properties of protein-coated surfaces at length scales ranging from tens of nanometers to millimeters. A silicon substrate is first coated with the extracellular matrix protein fibronectin, which is then locally inactivated by exposure to a highly focused electron beam. Biochemical inactivation of the protein is established by the loss of antibody binding to the fibronectin. Functional inactivation is determined by the inability of cells to spread or form focal adhesions on the inactivated substrate, resulting in cell shapes constrained to the pattern, while they do both (and are unconstrained) on the remaining fibronectin. These protein patterns have very high fidelity, and typical patterns agree with the input dimensions of the pattern to within 2%. Further, the feature edges are well defined and approach molecular dimensions in roughness. Inactivation is shown to be dose dependent with observable suppression of the specific binding at 2 μC cm^{-2} and complete removal of biochemical activity at $\sim$50 μC cm^{-2} for 5 keV electrons. The critical dose for inactivation also depends on accelerating voltage, and complete loss of antibody binding was achieved at $\sim$4$-$7 μC cm^{-2} for 1 keV electrons, which corresponds to $\sim$50$-$90 electrons per cross-sectional area of a whole fibronectin dimer and $\sim$2$-$4 electrons per type III fibronectin domain. AFM analysis of the pattern surfaces revealed that electron beam exposure does not remove appreciable amounts of material from the surface, suggesting that the patterning mechanism involves local inactivation rather than the ablation that has been observed in several organic thin film systems.

Introduction

Controlling the spatial distribution of proteins on nonbiological surfaces is important for a wide range of applications such as analytical and diagnostic protein arrays,[1−3] tissue engineering,[4] and biosensors.[5] Being able to construct surfaces with well-defined distributions of proteins also offers important capabilities for the study of fundamental aspects of cellular interactions with the extracellular environment. For the purpose of understanding how cells interpret spatially organized extracellular signals, the general approach has been to construct surfaces with a specific distribution of a protein, often an extracellular matrix protein, and then examine some functionally important consequence. For example, Thery and co-workers[6] recently showed that the axis of mitosis can be controlled by modulating cell shape using microcontact-printed patterns with dimensions on the order of tens of micrometers. Also, Chen et al. showed that cell shape governs cell growth and apoptosis by using patterned substrates to experimentally vary cell shape.[7] On a smaller length scale, the classic Massia and Hubbell result shows that for a fibroblast $\alpha_V\beta_3$ integrin interacting with an RGD peptide, the average spacing needed to support focal adhesion formation is 140 nm, while the average spacing needed to support cell spreading is 440 nm.[8] More recent work by Spatz and co-workers using methods that more uniformly control the spacing between molecules on the surface suggests that a critical dimension for integrin-mediated cell spreading lies in the range 58$-$73 nm.[9] Consistent with this finding, it has been proposed that the integrin-mediated binding requires a dimer in which

[†] Royal Institute of Technology.
[‡] Department of Physiology, Johns Hopkins School of Medicine.
[§] Department of Anesthesiology, Johns Hopkins School of Medicine.

(1) Zhu, H.; Snyder, M. *Curr. Opin. Chem. Biol.* **2001**, *5*, 40−5.
(2) Fang, Y.; Frutos, A. G.; Lahiri, J. *J. Am. Chem. Soc.* **2002**, *124*, 2394−5.
(3) Lynch, M.; Mosher, C.; Huff, J.; Nettikadan, S.; Johnson, J.; Henderson, E. *Proteomics* **2004**, *4*, 1695−702.
(4) Thissen, H.; Johnson, G.; Hartley, P. G.; Kingshott, P.; Griesser, H. J. *Biomaterials* **2006**, *27*, 35−43.
(5) Veiseh, M.; Zareie, M. H.; Zhang, M. Q. *Langmuir* **2002**, *18*, 6671−6678.
(6) Thery, M.; Racine, V.; Pepin, A.; Piel, M.; Chen, Y.; Sibarita, J. B.; Bornens, M. *Nat. Cell Biol.* **2005**, *7*, 947−53.
(7) Chen, C. S.; Mrksich, M.; Huang, S.; Whitesides, G. M.; Ingber, D. E. *Science* **1997**, *276*, 1425−8.
(8) Massia, S. P.; Hubbell, J. A. *J. Cell Biol.* **1991**, *114*, 1089−100.
(9) Arnold, M.; Cavalcanti-Adam, E. A.; Glass, R.; Blummel, J.; Eck, W.; Kantlehner, M.; Kessler, H.; Spatz, J. P. *ChemPhysChem* **2004**, *5*, 383−8.

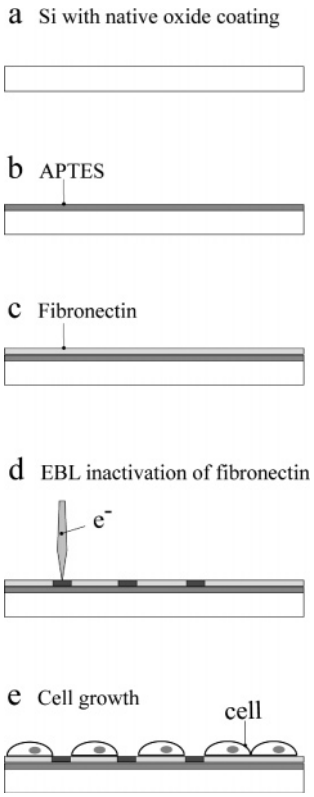

Figure 1. Schematic illustrating the electron beam approach for controlling the spatial distribution of protein activity. (a) A silicon substrate is cleaned, (b) coated with APTES to improve protein adsorption,[23] and then (c) coated with human fibronectin at surface-saturating concentrations. (d) The protein-coated surface is then patterned using a focused electron beam. (e) Cells are then grown on these patterns, and cellular responses to information in the patterns are studied.

the two binding sites are located ∼50 nm apart, at the ends of a talin complex.[10] There is also a substantial body of work on the role of membrane protein clustering in cell signaling.[11,12] Thus, protein organization at a length scale relevant in these types of experiments ranges from ∼10 nm to 100 μm.

A number of different methods for patterning proteins have been developed and employed,[13] such as microarray technology,[1] photolithography,[14] microcontact printing,[15] imprint lithography,[16] scanning probes,[17] and template patterns fabricated with energetic beams of X-rays and electrons.[18] These different methods all have strengths and weaknesses and are used as the particular application demands. Electron beam lithography (EBL) has three features that make it particularly useful for our interests. First, it is capable of patterning features as small as ∼5 nm and larger than square millimeters, and thus it spans the relevant length scale for cell−matrix interaction studies. Second, it is a writing technology that allows patterns to be changed very rapidly and flexibly. Third, the patterning can be dose dependent and can be used to produce gradients and other interesting non-binary features. Two approaches of protein patterning by EBL have been reported. First, EBL has been used to pattern self-assembled monolayers of molecules such as PEG by locally ablating the PEG. The ablated regions are then "backfilled" directly with a protein[19,20] or some chemical functionality that promotes subsequent binding of proteins to the surface.[21,22] Alternately, EBL has been used to produce gold patterns, which are used to constrain the distribution of proteins through a gold specific chemistry.[10] The latter approach exploits well-developed methods using standard EBL resists and lift-off processing although it also results in a protein pattern that is coupled to the topography and spatial distribution of the gold. Together these methods can be viewed as "additive" approaches, in which a pattern is used to confine or direct the attachment of protein to specific parts of a surface.

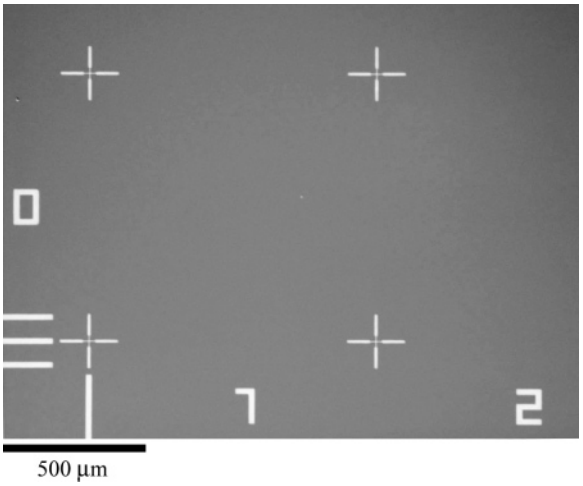

Figure 2. Light micrograph of the custom gold patterned substrates used in this work. This pattern provides index and guide marks for a 4 × 4 array of 1 × 1 mm^2 fields in the center of a 1 × 1 cm^2 silicon chip.

Here, we demonstrate a new approach for the fabrication of surfaces with a controlled distribution of the extracellular matrix protein fibronectin based on "erasing" the functionality of fibronectin coatings on a silicon surface by EBL. This is a writing approach that offers high flexibility with regard to the types of patterns that can be made and the speed with which they can be changed. In contrast to the previous approaches, this is a "subtractive" process in which a protein is first uniformly coated onto a surface and then locally inactivated by exposure to an electron beam (Figure 1). The proteins exposed to EBL show a dose-dependent decrease in affinity toward an anti-fibronectin antibody, while the unexposed protein remains functional by several criteria. Patterns have exceptionally well-defined edges and excellent fidelity with respect to the input pattern. The patterns can be used to encode information onto surfaces that living cells recognize and respond to.

(10) Cherniavskaya, O.; Chen, C. J.; Heller, E.; Sun, E.; Provenzano, J.; Kam, L.; Hone, J.; Sheetz, M. P.; Wind, S. J. *J. Vac. Sci. Technol., B* **2005**, *33*, 2972−2978.
(11) Thomason, P. A.; Wolanin, P. M.; Stock, J. B. *Curr. Biol.* **2002**, *12*, R399−401.
(12) Romer, L. H.; Birukov, K. G.; Garcia, J. G. *Circ. Res.* **2006**, *98*, 606−16.
(13) Blawas, A. S.; Reichert, W. M. *Biomaterials* **1998**, *19*, 595−609.
(14) Mooney, J. F.; Hunt, A. J.; McIntosh, J. R.; Liberko, C. A.; Walba, D. M.; Rogers, C. T. *Proc. Natl. Acad. Sci. U.S.A.* **1996**, *93*, 12287−12291.
(15) Xia, Y.; Whitesides, G. M. *Angew. Chem., Int. Ed.* **1998**, *37*, 550−575.
(16) Hoff, J. D.; Cheng, L.-J.; Meyhöfer, E.; Guo, L. J.; Hunt, A. J. *Nano Lett.* **2004**, *4*, 853−857.
(17) Wadu-Mesthrige, K.; Xu, S.; Amro, A.; Liu, G.-Y. *Langmuir* **1999**, *15*, 8580−8583.
(18) Mendes, P. M.; Preece, J. A. *Curr. Opin. Colloid Interface Sci.* **2004**, *9*, 236−248.
(19) Rundqvist, J.; Hoh, J. H.; Haviland, D. B. *Langmuir* **2006**, *22*, 5100−5107.
(20) Senaratne, W.; Sengupta, P.; Harnett, C.; Craighead, H.; Baird, B.; Ober, C. K. *Nanobiotechnology* **2005**, *1*, 23−33.
(21) Harnett, C. K.; Satyalakshmi, K. M.; Craighead, H. G. *Langmuir* **2001**, *17*, 178−182.
(22) Harnett, C. K.; Satyalakshmi, K. M.; Craighead, H. G. *Appl. Phys. Lett.* **2000**, *76*, 2466−2468.

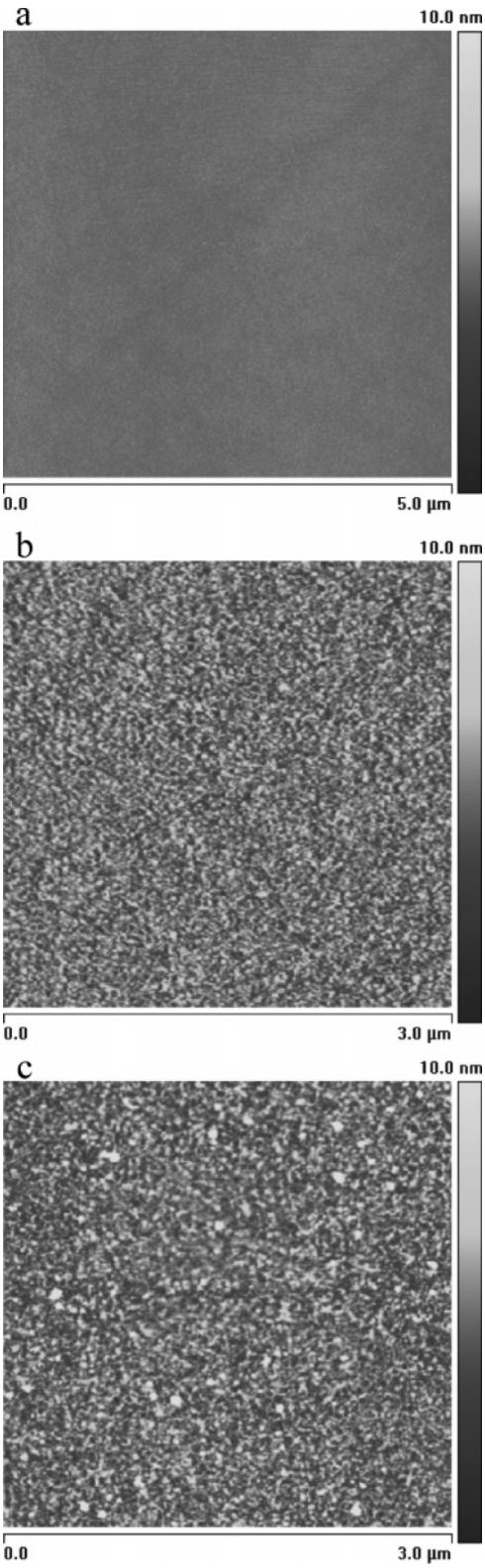

Figure 3. AFM images of substrates at different steps in the process of preparing fibronectin-coated surfaces. (a) The silicon substrates, cleaned with oxygen plasma, were contamination-free and had an rms roughness of 0.17 nm. (b) The APTES formed a uniform coating with an rms roughness of 0.8 nm. The APTES coating, completely covering the surface, was soft and could be scraped with an AFM tip. The thickness of the APTES coating was measured to 1.0 nm after locally removing the coating with the AFM tip by scraping and measuring the step height. (c) After the APTES surfaces had been coated with human fibronectin, the surface rms roughness increased to 1.47 nm and had randomly distributed aggregates with dimensions of many micrometers.

Experimental Section

Silicon Substrates with Gold Alignment Marks. It is important to be able to locate the patterned regions with high accuracy after the EBL. We therefore developed custom silicon substrates with gold alignment marks using a standard UV-based lift-off lithography process (Figure 2). The alignment marks consisted of 100 μm large gold crosses that divide the substrate into 16 1×1 mm^2 compartments in a 4×4 matrix, with guide lines on the edge of the main pattern. 500-μm-thick Si(100) wafers with a native oxide surface were scribed and cracked into a 3×3 matrix of 1×1 cm^2 chips. The whole matrix was processed simultaneously and cracked into individual 1×1 cm^2 chips after the final process step of EBL inactivation of the protein coating. The samples were first cleaned with an oxygen plasma in a reactive ion etch chamber (PlasmaLab 60, Oxford Instruments, Wiesbaden, Germany) to remove any organic contaminants from the silicon surface. For the lift-off lithography, silicon chips were first spin-coated with a UV-sensitive resist (Shipley S1818/EC solvent, 1:1 v/v, Micro Resist Technology GmbH, Berlin, Germany) and baked for 1 min at 100 °C. The resist thickness was measured to typically 410 nm. The resist was exposed to UV light through a mask with the alignment mark pattern using a contact mask aligner (model MJB3, Karl Süss, MicroTec Lithography GmbH, Munich, Germany) equipped with a Hg lamp (436, 405, and 365 nm). The exposed chips were developed for 25 s with Developer MF351 (Shipley)/MilliQ water (>18 MΩ cm) 1:3.375 v/v and then rinsed in MilliQ water for 45 s and finally dried by gently blowing with compressed nitrogen. A 2 nm thick titanium adhesion layer followed by a ~50 nm gold layer were then deposited by electron gun evaporation (base pressure 2×10^{-7}). After deposition, the gold was lifted-off by dissolving the resist with acetone. Substrates were then rinsed with MilliQ water and dried with compressed nitrogen.

Protein-Coated Silicon Substrates. The substrates were first immersed into a piranha solution (H_2SO_4/H_2O_2, 2:1 v/v) at room temperature for 15 min to obtain a clean surface with hydroxyl groups. The chips were then carefully rinsed with MilliQ water for at least 10 min and dried under a stream of nitrogen. To facilitate protein adsorption,[23] the substrates were then immersed into an ethanolic 3-aminopropyltriethoxysilane (APTES; Gelest, Inc., Morrisville) solution (ethanol 99.5%/APTES 99+%, 10:1 v/v) overnight (typically ~15 h). After incubation, the chips were washed with ethanol under agitation by a shaking table and blown dry under a stream of nitrogen. Finally, the chips were cured in an oven at 110 °C for 5 h.

The APTES-coated substrates were incubated with human fibronectin (Invitrogen, via VWR International, Stockholm, Sweden). A 300 μL drop of 150 mM NaCl, 5 mM Tris-HCl, 0.1% w/v NaN_3, pH 7.6 (UB), was placed on a piece of Parafilm, and then 200 μg of fibronectin from a 1 mg/mL stock solution was added to the droplet and carefully mixed using a pipet. The APTES-coated chip was placed onto the droplet with the APTES side facing down toward the droplet. This procedure minimized evaporation during incubation. The chip was incubated for approximately 18 h. After incubation the chip was carefully lifted from the droplet and first washed with UB and then with MilliQ water before drying under a stream of nitrogen.

Electron Beam Patterning. The fibronectin-coated chips were patterned by EBL using a Raith 150 Turnkey system with a high precision interferometric stage (Raith GmbH, Dortmund, Germany). The chips were exposed with the accelerating voltage set to 1, 5, or 25 kV with a 30 μm aperture and a beam current of 0.12, 0.15, and 0.24 nA, respectively, at a working distance of ~5.5 mm. The patterns were written with a 20 nm step size, and the dose was controlled by the time spent at each pixel (0.1 μs resolution). The chamber pressure was $(2.1-2.3) \times 10^{-7}$ mbar during exposures, and the chips were typically exposed to the vacuum for up to 12 h. The effect of electron irradiation dose on the fibronectin was tested by exposing rectangular areas of

(23) Cunliffe, D.; Smart, C. A.; Alexander, C.; Vulfson, E. N. *Appl. Environ. Microbiol.* **1999**, *65*, 4995−5002.

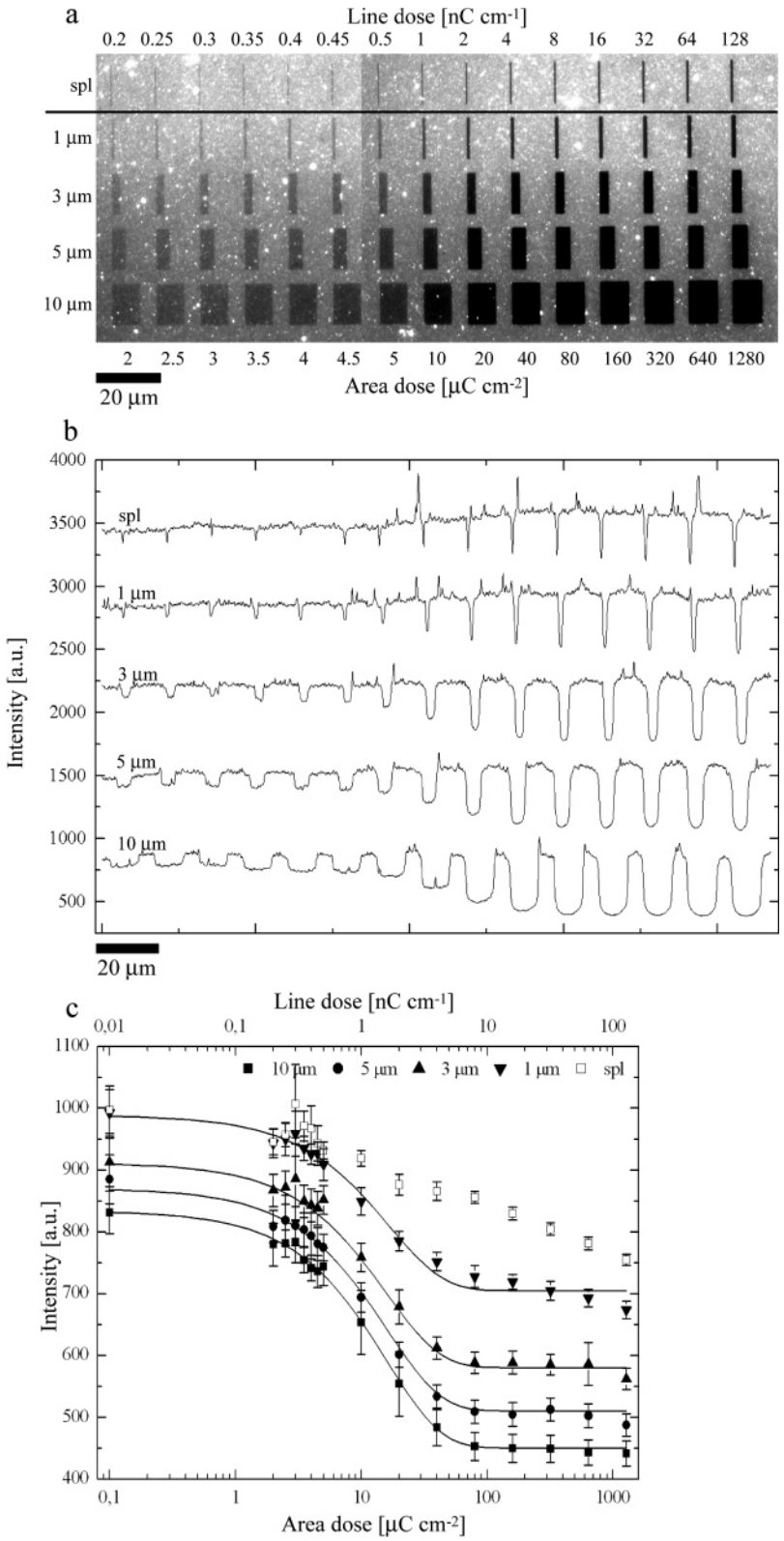

Figure 4. EBL dose test of exposure of fibronectin at 5 kV accelerating voltage. (a) The fibronectin-coated surface was exposed by EBL in the shapes of rectangles of different widths, and single pixel lines (spl), at doses ranging from 2 to 1280 μC cm^{-2} and subsequently stained with an antibody against fibronectin (and a fluorescent secondary antibody against the primary antibody). The stained fibronectin appears bright with some spots of high intensity, likely small aggregates of the protein. There is some variation in intensity over the captured images due to uneven illumination from the excitation source and photobleaching of the fluorophores. Binding of the anti-fibronectin antibody to the fibronectin is suppressed by electron irradiation in a dose-dependent fashion. The image is a composite of several experiments, and the contrast in the fluorescence micrographs was adjusted for presentation purposes. (b) Intensity profiles for the dose test. The intensity profile for each feature size was measured by averaging the horizontal lines over the whole height of the rectangles of each width. The dose-dependent inactivation apparent in (a) is clearly seen. Profiles for different feature widths have been shifted for clarity. (c) Dependence of inactivation on dose. To quantify the inactivation dependency on dose, a histogram of all of the pixels in a feature was produced, and the mean pixel intensity within a feature was determined and plotted versus electron dose.

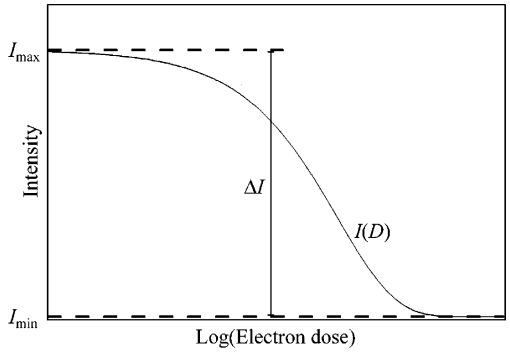

Figure 5. Illustration of the exponential decay function used in the analysis of the dose response data.

width 10, 5, 3, and 1 μm as well as single pixel lines to electron doses ranging from 1 to 1280 μC cm^{-2}. The total exposure time for these test patterns was ~40 min.

Atomic Force Microscopy. The surfaces were analyzed using a MultiMode atomic force microscope (AFM) system with a J-scanner and a NanoScope IV or NanoScope IIIa controller (Veeco Metrology Group, Digital Instruments, Santa Barbara, CA). The dry samples were imaged by contact mode AFM using oxide-sharpened silicon nitride probes (Olympus OTR4 or Microlevers, Veeco Metrology Group) with nominal spring constants ~0.08 N/m (OTR4) or 0.03 N/m (Microlevers). The raw data were processed with the NanoScope software by second-order plane-fit and first-order flattening.

Cell Culture and Plating on Fibronectin Patterns. Swiss 3T3 cells were grown in Dulbecco's Modified Eagle Media (Invitrogen, Carlsbad, CA) with 10% fetal bovine serum (Atlanta Biologicals, Lawrenceville, GA) at 37 °C and 5% CO_2. Cells were passaged every 3−4 days using trypsin-EDTA (Invitrogen). Cells were resuspended in serum free media before being applied to the patterned surface. Three hours after plating, the cells were fixed with ice-cold 3% paraformaldehyde (Sigma, St. Louis, MO).

Immunofluorescence. The samples were stained for fibronectin with a primary polyclonal rabbit anti-human fibronectin antibody (ab299, Abcam, Cambridge, MA), and then an AlexaFlour-448-labeled anti-rabbit secondary antibody from goat (Invitrogen). The cell membrane and the nucleus were stained with 1-1′-dioctadecyl-3,3,3′,3′-tetramethylindocarbocyanine perchlorate (DiI, Invitrogen) and 4′,6-diamindino-2-phenylindole, dihydrochloride (DAPI, Invitrogen), respectively. Vinculin was stained with a monoclonal anti-vinculin antibody (clone 7F9; gift from Dr. Alexey Belkin, University of Maryland School of Medicine, Baltimore, MD), and a Cy5 labeled anti-mouse secondary antibody (Jackson Laboratories, Bar Harbor, ME). After staining, the samples were mounted onto a coverslip using FluorSave (EMD Biosciences, Inc., San Diego, CA). Fluorescence images of the samples were taken using a Nikon epifluorescence microscope with a 60× objective, a 12-bit cooled CCD camera (CoolSnap HQ, Photometrics, Tuscon, AZ), and image acquisition software (OpenLab, Improvision, Lexington, MA). The subsequent images were combined and processed using Adobe Photoshop (Adobe, San Jose, CA).

Results and Discussion

Spatially Controlled Dose-Dependent Inactivation of Fibronectin. The fibronectin-coated surfaces appeared to be uniformly coated and had an rms roughness of 1.47 nm. There was occasional particulate matter that appeared to be aggregated protein (Figure 3). Prior to patterning, these substrates bound antibodies to fibronectin and supported normal spreading and focal adhesion formation by Swiss 3T3 cells (not shown). Exposing the protein coating to a highly focused electron beam resulted in a biochemical and functional inactivation of the fibronectin. Biochemical inactivation was determined by the loss of binding to a polyclonal antibody against fibronectin, established by immunofluorescence microscopy. Functional inactivation was determined by the inability of cells to spread or form focal adhesions on the inactivated substrate. Antibody binding was used as the primary assay for determining the patterning parameters and patterning mechanisms. Functional cell-based studies, described below, were performed on substrates patterned using parameters established using antibody binding.

To characterize the patterning conditions, a series of test patterns were produced with varied feature size and dose. These patterns were exposed, stained, and visualized by immunofluorescence microscopy. The fluorescence intensity was taken to be proportional to the biochemical activity of the fibronectin. The biochemical inactivation was determined as a function of exposure dose for patterns of different sizes using 1, 5, and 25 keV electrons. Qualitatively, the results for all three cases are similar. Here, the case for 5 kV acceleration voltages is presented in some detail, and the effects of accelerating voltage are considered below. For the 5 kV test patterns, all exposure doses decreased biochemical activity (Figure 4a) including the lowest dose (2 μC cm^{-2}). There is a clear dose dependence; as the electron dose increases, the binding of the antibody to the fibronectin decreases, resulting in a gradual decrease in labeling intensity of the exposed areas (Figure 4a). The decrease in intensity is seen for all feature widths (10, 5, 3, 1 μm wide rectangles and single pixel lines).

To establish the critical dose, beyond which no further biochemical inactivation occurs, intensity histograms for each exposed area, as well as unexposed areas, were examined (Figure 4c). The resulting data have the form of an exponential decay and, for each feature width (except single pixel lines, which were not sufficiently well resolved), were fit to the function:

$$I(D) = I_{min} + (I_{max} - I_{min})e^{-D/\gamma} \quad (1)$$

Here, $I(D)$ is the measured intensity at some dose D, and γ is a constant unique for each curve. I_{min} and I_{max} are the minimum and maximum intensity values that are approached by the curves as the dose approaches zero and infinity, respectively (dashed lines in Figure 5). The analysis performed here has an analogue in EBL exposures of polymeric thin film resists where film retention, instead of intensity, is plotted versus electron dose.[24] Equation 1 gives an expression for D,

$$D(I) = -\gamma \ln\left(\frac{I - I_{min}}{\Delta I}\right) \quad (2)$$

where $\Delta I = I_{max} - I_{min}$. Using eq 2, the critical dose D_c required for biochemical inactivation of the protein-coated surface was determined. The threshold for the critical dose ($D_c \equiv D(I_c)$) was taken to be 5% of ΔI from I_{min} ($I_c \equiv 0.05\Delta I + I_{min}$), and the D_c for each feature width was calculated (Table 1). The critical dose for 5 kV exposures was calculated to ~45−50 μC cm^{-2} for 10, 5, 3, and 1 μm wide rectangles. The variation in I_{min} and I_{max} for the different curves is caused by the uneven illumination from the excitation lamp in the fluorescence microscope, which, however, does not affect the value of γ.

(24) Rai-Choudhury, P. *Microlithography, Micromachining, and Microfabrication, Volume 1: Microlithography*; SPIE Press: Bellingham, WA, 1997.

Table 1.

	accelerating voltage					
	5 kV			1 kV		
width [μm]	constant (γ) [cm^2 μC^{-1}]	error (σ) [cm^2 μC^{-1}]	$D(0.05\Delta I + I_{min})$ [μC cm^{-2}]	constant (γ) [cm^2 μC^{-1}]	error (σ) [cm^2 μC^{-1}]	$D(0.05\Delta I + I_{min})$ [μC cm^{-2}]
10	16.1	0.701	48.3	2.31	0.192	6.92
5	15.1	0.824	45.2	1.21	0.170	3.62
3	16.7	1.31	49.9	1.10	0.190	3.31
1	16.7	2.02	50.0	1.29	0.350	3.88

Low Accelerating Voltages Are More Effective for Inactivation. Similar dose tests were performed using 1 and 25 kV accelerating voltages. The 1 kV results are qualitatively identical to the 5 kV results, with decreasing fluorescence intensity as the electron dose increases. However, in the 1 kV case, the biochemical inactivation occurs at significantly lower doses; this higher efficiency of inactivation results in a lower critical dose (Figure 6b,c). We note that the critical dose for 1 kV exposures was ~4 μC cm^{-2} for 10, 5, and 3 mm rectangles and ~7 μC cm^{-2} for 1 μm rectangles (Figure 6c). This corresponds to 50−90 electrons per whole fibronectin molecule (assuming a molecular cross-sectional area of 200 nm^2), or 2−4 electrons per type III fibronectin domain (assuming a molecular cross-sectional area of 10 nm^2).[25,26] The data for the single pixel lines were too scattered to fit a curve and extract a critical dose. In the 25 kV case, there is again dose dependence, but inactivation occurs at doses well above those for both 5 and 1 kV (data not shown). Thus, within the range of voltages examined, the lowest acceleration voltage is the most effective at inactivation, and the highest is the least effective. This dependence on accelerating voltage suggests that inactivation is due in large part to secondary electrons being absorbed in the surface layer at low incident beam energy. When the electrons strike the vacuum−solid interface, several processes occur that involve primary, backscattered, and secondary electrons. At higher energies, the penetration depth of the primary electrons is larger (several micrometers for 25 keV electrons in silicon)[23] than for lower energy electrons. When the primary and backscattered electrons slow down, much of their energy is dissipated as secondary electrons with energies from 2 to 50 eV. The secondary electrons act on a range up to 20 nm and are responsible for the bulk exposure process in electron resists and, likely, also in our system with the protein coating.[23] At large primary penetration depths, the secondary electrons do not interact with the surface coating. We note that common covalent bonds in proteins have energies of ~3−4 eV.[27] Further, studies on electron beam-based functional inactivation of proteins in solution have shown that energies of ~60 eV (transferred via inelastic scattering) can produce complete loss of protein activity.[28] Thus, energies of the secondary electrons are in a range where the breaking of covalent bonds in proteins would be expected.

EBL Patterning of Fibronectin Does Not Entail Appreciable Ablation. To gain insight into the mechanism of patterning, EBL patterned fibronectin substrates were imaged by AFM. Previous studies of EBL patterning of organic thin films, for example PEG SAMs, have shown that electron beam exposure results in physical removal of material from the exposed areas.[20] However, AFM images of the EBL patterned fibronectin surfaces show no detectable change in the surface topography, and thus no detectable pattern (Figure 7a). AFM imaging following a water rinse likewise exposed no visible topography (data not shown). Staining of the same samples revealed antibody labeling by both immunofluorescence (e.g., Figures 4a and 6a) and AFM imaging (Figure 7b), where the topography of the pattern appeared only after staining. Here, the gold alignment marks on the substrate were particularly important to ensure that the same area was being examined before and after staining. Thus, the patterning mechanism here is a novel one that involves the functional inactivation of proteins without appreciable mass removal. One advantage of this mechanism is that it does not introduce a topographic component to the pattern, which could confound analysis of cellular responses because some cell types have been shown to respond to nanometer scale topographic features.[29]

The chemical nature of the material left after EBL exposure is at present not known. However, we note that the characteristic size of a protein epitope recognized by an antibody is ~6 amino acids (for linear epitopes).[30] Further, one of the critical peptides within fibronectin is the RGD tripeptide, which supports the cell spreading and formation of focal adhesions.[31] To achieve complete loss of antibody binding or loss of RGD-based function, there must therefore be electron-induced damage within any stretch of 3−6 amino acids within the fibronectin molecule. The precise location of this damage is uncertain, but the side chains contain the majority of the bonds within a protein molecule. It is likely that a significant fraction of the side chains within the protein are damaged at the critical doses established here. The peptide backbone will also be damaged, although at a lower frequency than the occurrence of damaged side chains.

High Pattern Fidelity. Patterning fidelity was evaluated by comparing the input pattern used to control the EBL with AFM images of stained pattern surfaces (Figure 8a). This comparison demonstrates excellent agreement between the two, with a mean deviation from the input pattern as high as 8% for some 1 μm features (i.e., 80 nm), but typically 2% or less of the feature dimensions. Pattern edges were examined by measuring the average height across a feature boundary (Figure 8b). The edge sharpness was defined as the distance corresponding to 90% of the step height and is typically 60−150 nm. The dimensions of a fibronectin dimer vary depending on the conditions under

(25) Erickson, H. P.; Carrell, N. A. *J. Biol. Chem.* **1983**, *258*, 14539−44.
(26) Leahy, D. J.; Aukhil, I.; Erickson, H. P. *Cell* **1996**, *84*, 155−64.
(27) Atkins, P. *Physical Chemistry*, 5th ed.; Freeman and Co.: New York, 1994; p 1031.
(28) Ronan, R. S.; Heinz, W. F.; Kempner, E. S. *Radiat. Environ. Biophys.* **1996**, *35*, 159−62.
(29) Curtis, A. S.; Casey, B.; Gallagher, J. O.; Pasqui, D.; Wood, M. A.; Wilkinson, C. D. *Biophys. Chem.* **2001**, *94*, 275−83.
(30) Appel, J. R.; Pinilla, C.; Niman, H.; Houghten, R. *J. Immunol.* **1990**, *144*, 976−83.
(31) Ruoslahti, E. *Annu. Rev. Cell Dev. Biol.* **1996**, *12*, 697−715.

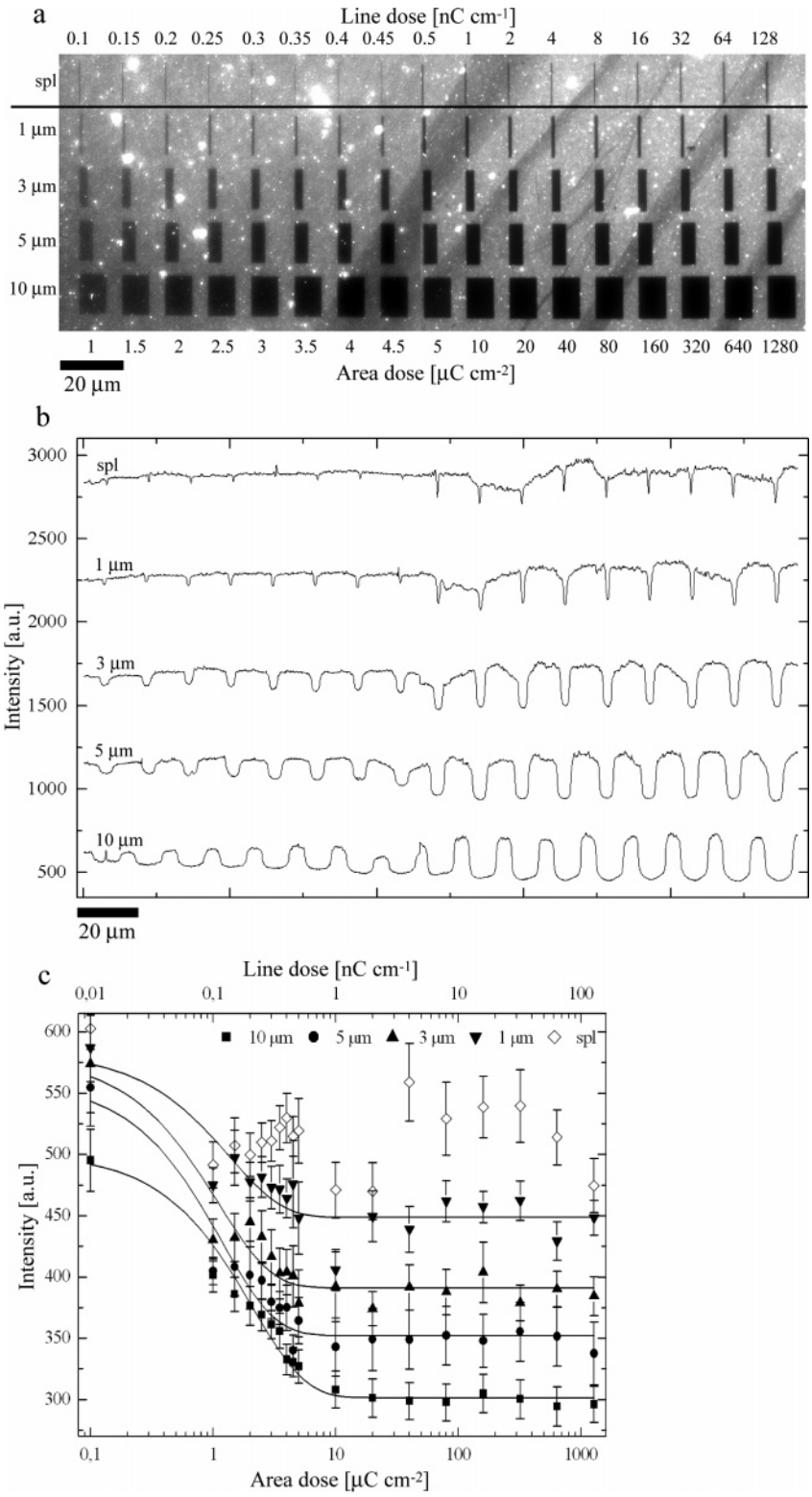

Figure 6. EBL dose test of exposure of fibronectin at 1 kV acceleration voltage. (a) Fluorescence micrographs of dose series for different shaped features. Conditions are identical to those in Figure 4. (b) Intensity profiles for the dose test. (c) Dependence of inactivation on dose. The findings for 1 kV qualitatively parallel those from 5 kV with the notable exception that the inactivation occurs at a much lower dose at 1 kV.

which it was deposited, with its long axis in the range 50−100 nm.[25] On hydrophobic surfaces of the type used here, fibronectin will generally take on the more compact form.[32] Thus, the edges have a sharpness approaching molecular dimensions. Antibody binding is a stochastic process and may itself introduce noise; therefore, the sharpness presented here likely represents an upper bound.

EBL Patterns of Fibronectin Are Functional. To demonstrate that the patterns produced by EBL are functional, we plated Swiss 3T3 fibroblasts on specific patterns of fibronectin.

(32) Bergkvist, M.; Carlsson, J.; Oscarsson, S. *J. Biomed. Mater Res., A* **2003**, *64*, 349−56.

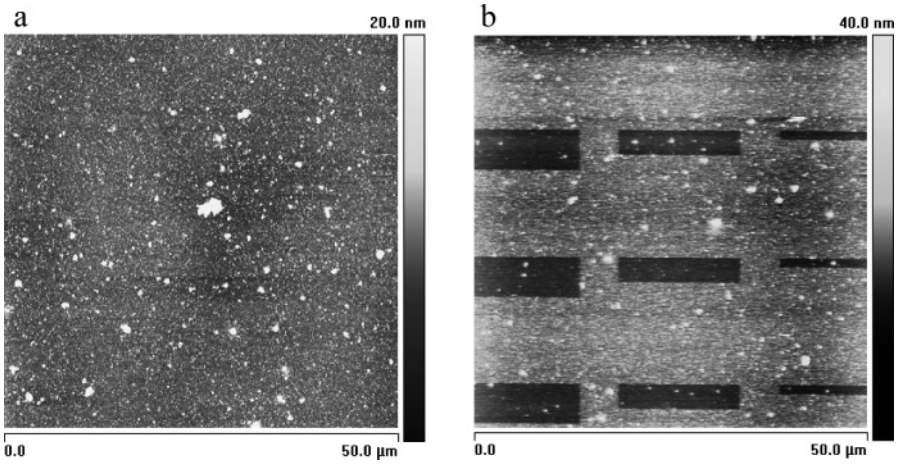

Figure 7. Characterization of the electron beam exposed fibronectin by AFM. (a) Contact mode AFM image of an EBL exposed fibronectin-coated substrate shows no detectable pattern. The input pattern is of similar shape to the one used in Figures 4 and 6, except that no single lines were used. (b) The same sample after staining with a primary antibody for fibronectin and a secondary fluorescent antibody. This staining reveals a clear pattern in the AFM image.

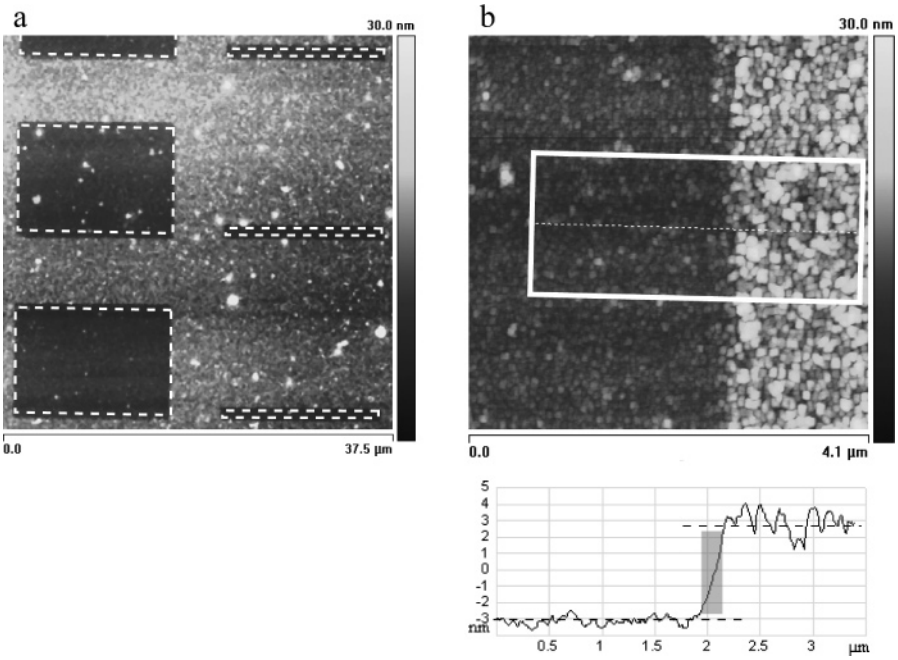

Figure 8. Characterization of pattern fidelity and edge sharpness by AFM. (a) Comparison of the programmed input pattern (white dashed squares) with an AFM image of the protein pattern shows excellent agreement between the two. Analysis of the deviation between the two reveals it to be as high as 8% for 1 μm features but typically 2% or less for larger features, with the protein pattern being slightly larger than the input pattern. (b) Close examination of a feature definition shows that the edges are exceptionally sharp. The average height profile of the step in this example is 90% of the height change over <60 nm. This is close to the dimensions of the compact form of the fibronectin dimer (50 nm).

In these experiments, cells were trypsinized and plated onto patterned surfaces for 2−4 h before being fixed and stained. Fluorescence microscopy revealed that cells spread well on the patterned surfaces although they avoided areas inactivated by electron beam exposure and were strongly confined to the pattern of fibronectin (Figure 9a−c). Indeed, the pattern in many instances determined the shape of the cell. Immunological staining for vinculin (a widely used marker for focal adhesions) revealed the staining characteristic of focal adhesions (Figure 9d), further demonstrating that these substrates are functionally competent to support normal cell surface interactions seen on fibronectin-coated surfaces. Several other cell types, including B16 melanoma cells and mouse embryonic fibroblasts, likewise show spreading and confined growth on patterned substrates (data not shown). Thus, the patterned fibronectin on these substrates supported functionality in a manner that was similar to fibronectin coated on glass coverslips or plastic, two widely used substrates in cell biological research.

Limitations of the EBL Approach. One significant limitation of the electron beam-based approach is that proteins must retain activity after exposure to vacuum for many hours. Some proteins, such as fibronectin, clearly do this, and there are many proteins that can be lyophilized and subsequently rehydrated. Further, many, if not most, short peptides can be dried and rehydrated to functional states repeatedly. However, there will also be many proteins for which this approach is not suitable. Thus, the approach is not completely general, as is the case for most patterning approaches. Another limitation is that, as described, one can only pattern one type of molecule, and many interesting problems require two or more different molecules in different patterns on the surface. One approach to overcoming this problem is serial EBL as described by Harnett et al.,[22] in

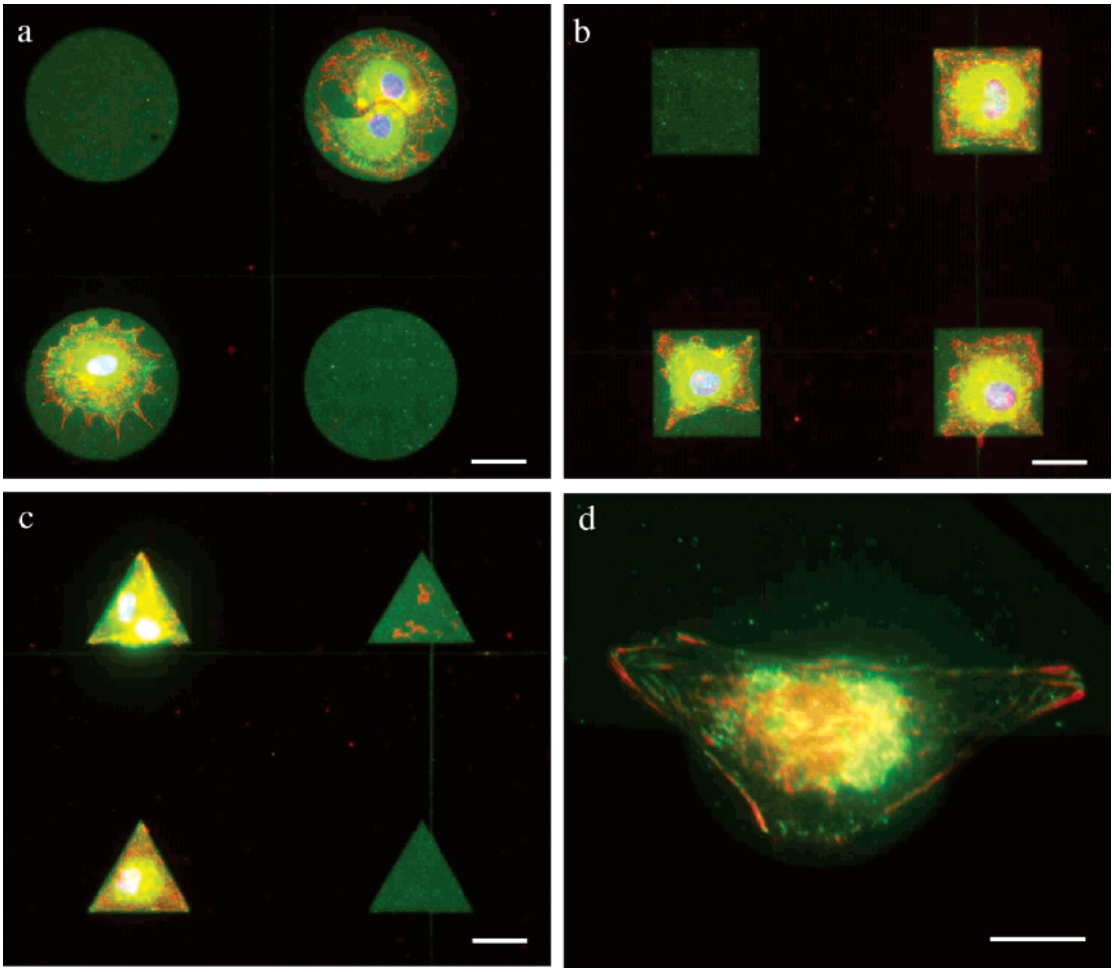

Figure 9. Characterization of pattern functionality using Swiss 3T3 cells. (a)−(c) The optimal writing parameters (1 kV accelerating voltage and 20 μC cm^{-2}) were used to produce fibronectin (green) patterns of squares, triangles, and circles. Cells grown on the different shapes are constrained by the shape of the protein pattern. The cells avoid growing into the EBL exposed areas but spread well on the remaining fibronectin. In addition, cell membranes are stained with DiI (red) and nuclei stained with DAPI (blue). (d) Staining for vinculin (red) as a marker for focal adhesions demonstrates that the cells form functional contacts with the fibronectin. Here, the membrane and nuclear staining is omitted. Scale bars are 25 μm.

which a patterned surface is subjected to additional rounds of EBL exposure followed by backfilling. However, in this approach the first pattern is likely to be contaminated by the subsequent molecules used for backfilling. It also requires accurate registration of patterns, which is possible for EBL to $<$20 nm. One way to circumvent the contamination problem and to produce multicomponent patterns would be to produce larger scale multicomponent patterns using other means, such as, for example, microfluidic approaches, followed by EBL to edit these patterns. Finally, patterning time is a limitation compared to some other methods. The precise time to produce patterns using the approach described here depends on a large number of factors and is not easily described. However, in practice we routinely make simple geometric patterns where approximately one-half the area is EBL exposed at a rate of $\sim$1 mm^2 per hour. 1 mm^2 is enough for tens to hundreds of cells to attach to, and thus the approach will be useful for many types of interesting experiments.

Conclusions

The patterning approach described here is likely to be widely applicable to the extent that many or most types of proteins can likely be functionally inactivated by electron irradiation at doses similar to those for fibronectin. Further, this is a writing approach that is highly flexible with a large dynamic range, effectively covering large and small areas, and is suitable for quickly changing patterns in response to experimental demands. Previous work on EBL of the organic polymer PEG shows that feature sizes of $\sim$40 nm can be achieved, and the features here have edges with dimensions approaching those of individual protein molecules. With a better understanding of the patterning conditions and the biophysical details of matrix protein inactivation, there are excellent prospects for improving patterning resolution. It is likely that functional inactivation by electron beam exposure will allow for patterning proteins at the single molecule level in many systems.

Acknowledgment. This work was supported in part by a grant from the Swedish Foundation for Strategic Research Bio-X Program (D.B.H.), grants from the National Institutes of Health R21HL76241 (J.H.H.) and AI061042 (L.H.R.), and the Fund for Medical Discovery at Johns Hopkins University (L.H.R.). The samples used in this work were produced in the KTH NanoFabLab funded by the Knut and Alice Wallenberg Foundation. We also thank Devrim Pesen for her help with AFM imaging and helpful suggestions.

JA063698A